Structural investigation of the covalent and electrostatic binding of yeast cytochrome c to the surface of various ultrathin lipid multilayers using x-ray diffraction

James M. Pachence and J. Kent Blasie
Chemistry Department, University of Pennsylvania, Philadelphia, Pennsylvania 19104 USA

ABSTRACT X-Ray diffraction was used to characterize the profile structures of ultrathin lipid multilayers having a bound surface layer of cytochrome c. The lipid multilayers were formed on an alkylated glass surface, using the Langmuir-Blodgett method. The ultrathin lipid multilayers of this study were: five monolayers of arachidic acid, four monolayers of arachidic acid with a surface monolayer of dimyristoyl phosphatidylserine, and four monolayers of arachidic acid with a surface monolayer of thioethyl stearate. Both the phosphatidylserine and the thioethyl stearate surfaces were found previously to covalently bind yeast cytochrome c, while the arachidic acid surface electrostatically binds yeast cytochrome c. Meridional x-ray diffraction data were collected from these lipid multilayer films with and without a bound yeast cytochrome c surface layer. A box refinement technique, previously shown to be effective in deriving the profile structures of ultrathin multilayer lipid films with and without electrostatically bound cytochrome c, was used to determine the multilayer electron density profiles. The surface monolayer of bound cytochrome c was readily apparent upon comparison of the multilayer electron density profiles for the various pairs of ultrathin multilayer films plus/minus cytochrome c for all cases. In addition, cytochrome c binding to the multilayer surface significantly perturbs the underlying lipid monolayers.

INTRODUCTION

Cytochrome *c* is a relatively small peripheral membrane heme protein that interacts with a number of integral membrane electron transfer proteins (2). For example, cytochrome *c* has been shown to bind to both the cytochrome bc_1 complex and cytochrome *c* oxidase in its participation in the electron transfer reactions of the mitochondrial inner membrane. In addition, cytochrome *c* interacts strongly with lipid monolayer and bilayer systems (1–3, 13). The elucidation of the structural nature of these various interactions is important for understanding the mechanism of electron transfer among these membrane associated proteins.

Recently, we have fabricated a membrane system consisting of an ultrathin fatty acid multilayer film, formed via the Langmuir-Blodgett technique, possessing a surface monolayer of electrostatically bound horse heart cytochrome *c* (4–6). Previous structural studies have firmly established the position of this electrostatically bound cytochrome *c* surface monolayer with respect to the profile structure of these ultrathin lipid multilayer films, using both nonresonance and resonance x-ray diffraction (5, 6). In addition, optical linear dichroism was used to determine the orientation of the heme group of electrostatically bound horse heart cytochrome *c* or covalently bound yeast cytochrome *c* on the surface of ultrathin lipid multilayer films (4). The orientation of the heme group of the bound cytochrome *c*, coupled with the previously derived structural information, showed that this lipid multilayer film/protein surface monolayer system provides a vectorially oriented cytochrome *c* which could be used as a ligand to bind membrane associated electron transfer proteins such as photosynthetic reaction centers (4–6).

This study extends the previous structural studies to include the profile structures of ultrathin lipid multilayer films having a surface monolayer of dimyristoyl phosphatidylserine or thioethyl stearate (TES) to which yeast cytochrome *c* can be covalently bound (as obtained via nonresonance x-ray diffraction). It has been previously found that a cysteine residue on yeast cytochrome *c* located near the carboxy-terminus at sequence position 102 forms a covalent linkage spontaneously with the thiol moiety of TES, or with the amine moiety of phosphatidylserine (4, 7). Comparisons are made between the results of these structural studies and the results from our previous cytochrome *c*/lipid multilayer studies. In particular, the utilization of the covalent complex of TES and yeast cytochrome *c* is discussed as a vehicle to study the supramolecular organization of biomolecular complexes of cytochrome *c* with integral membrane proteins, such as cytochrome oxidase, cytochrome bc_1, or photosynthetic reaction centers.

MATERIALS AND METHODS

Flat glass plates ($11 \times 25 \times 1$ mm^3) were coated with octadecyltrichloro- silane (OTS, Aldrich Chemical Co., Milwaukee, WI), according to the method by J. Sagiv (8) to form a hydrophobic substrate surface. Arachidic acid (Aldrich Chemical Co.) was zone refined with 50 zone passes at a rate of 1 cm/h and the purity of the

0006-3495/91/04/894/07 $2.00

center fraction confirmed by Differential Scanning Calorimetry (DSC) measurements (DuPont 990, Wilmington, DE). Dimyristoyl phosphatidylserine was purchased from Avanti Polar Lipids Inc. (Birmingham, AL). Mercaptoethanol, methyl methane thiosulfonate, stearic acid, stearic anhydride, and pyridine were products of Aldrich. Yeast cytochrome *c* from Saccharomyces cerevisiae was obtained from Sigma Chemical Co. (St. Louis, MO).

The thioethyl ester of stearic acid with a protected sulfhydryl group, namely thiomethyl-thioethyl stearate, was synthesized. The procedure was essentially that of Ganong and Bell (9), with modifications to synthesize a thiol-fatty acid ester vs. the phosphatidyl- thioglycerol of the original report (4). Lipid monolayers (arachidic acid, thiomethyl-thioethyl stearate, and dimyristoyl phosphatidylserine) were deposited onto the alkylated glass substrates via the Langmuir-Blodgett technique at the constant surface pressure of 20 dyne/cm, as described previously (5). Four monolayers of arachidate were deposited onto each substrate; a final surface monolayer consisting of arachidic acid, thiomethyl-thioethyl stearate, or phosphatidylserine was then deposited (with the subphase surface being cleaned before the formation of the thiomethyl-thioethyl stearate or phosphatidylserine monolayers). The resulting hydrophilic film surface was always thereafter in contact with the polar solvent, with the final buffer being 1 mM $NaHCO_3$ at pH 8.

The Langmuir-Blodgett multilayer films containing a surface monolayer of thiomethyl-thioethyl stearate were activated before use by removing the thiomethyl group. This was done by placing the glass slide substrate into a glass vial containing the 1 mM $NaHCO_3$, pH 8.0 ± 0.2, and 0.1 mM dithiothreitol for 1 h. The supernatant was then replaced with 1 mM $NaHCO_3$, pH 8.0 + 0.2 three times before combining with cytochrome *c*.

Ultrathin multilayer films consisting of five lipid monolayers (with surface of arachidic acid, thioethyl stearate, or phosphatidylserine) were incubated for 48 h or more in 10 μM yeast or horse heart cytochrome *c* solution in 1 mM $NaHCO_3$, pH 8. Each film was removed from the cytochrome *c* solution, and incubated with 1 mM $NaHCO_3$ buffer for 2 h or more. The buffer was changed every 5 min until there was no detectable cytochrome *c*, measured spectrophotometrically in the supernatant. The glass slide substrate supporting the ultrathin multilayer films was then suspended in a quartz cuvette (1 cm path length), containing a solution of 1 mM $NaHCO_3$ and between 0.01 and 0.1 mM Ascorbate (to reduce the cytochrome *c*) at pH 8, and the optical absorption spectra were recorded with a double beam spectrophotometer to determine the amount of bound cytochrome *c* (4).

Meridional x-ray diffraction was obtained from the multilayers as a function of $q_z = (2 \sin \theta)/\lambda$, corresponding to elastic photon momentum transfer along the *z*-axis, perpendicular to the substrate plane. This meridional x-ray diffraction arises from the projection of the three-dimensional multilayer electron density distribution along radial vectors lying in the layer planes perpendicular to the *z*-axis onto the *z*-axis; the projection is defined as the electron density profile for the multilayer. The incident x-ray beam defines an angle omega (ω) with the substrate plane (*x*-*y*). Meridional x-ray diffraction is observed for ω equal to θ, where 2θ is the angle between the incident and scattered beams. The multilayers were therefore positioned on the ω axis of a two-axis Huber diffractometer which was scanned over an appropriate range of ω values permitting the collection of meridional diffraction data with a low impedance position-sensitive detector (PSD) aligned along the q_z direction and mounted on the 2θ axis. An Elliott (GX-6) rotating anode x-ray generator was used to produce the incident Cu K_α x-rays at a target loading of ~2.5 KW/mm². K_α x-rays were selected with a nickel filter and line focused parallel to the ω-axis at the PSD entrance window using Franks' optics. The wet lipid multilayer films with or without cytochrome *c* were equilibrated in a helium atmosphere of 98% relative humidity, and all samples were maintained at room temperature during the experiment.

Details regarding ω-scan parameters have been outlined previously (5). Each ω-scan required ~10 h, resulting in an oscillation pattern which represents the meridional intensity function $I(q_z)$. Each intensity function was corrected for background scattering followed by a Lorentz correction of q_z to correct for oscillation of the multilayers in the ω-scan to yield the corrected intensity function $I_c(q_z)$.

RESULTS

It was previously determined from the optical absorption spectra of the various ultrathin lipid multilayer films pre-incubated with cytochrome *c* that the amount of protein bound to the surface was consistent with a close packed monolayer bound to the lipid multilayer film surface (4, 5). It was also shown that the interaction between yeast cytochrome *c* and the arachidic acid surface was mainly electrostatic, while the interaction between yeast cytochrome *c* and either TES or phosphatidylserine was covalent (4, 5).

Meridional x-ray diffraction data from each ultrathin multilayer film, plus/minus a bound surface layer of yeast cytochrome *c*, were collected: Fig. 1 shows the corrected intensity data $I_c(q_z)$ for the ultrathin films

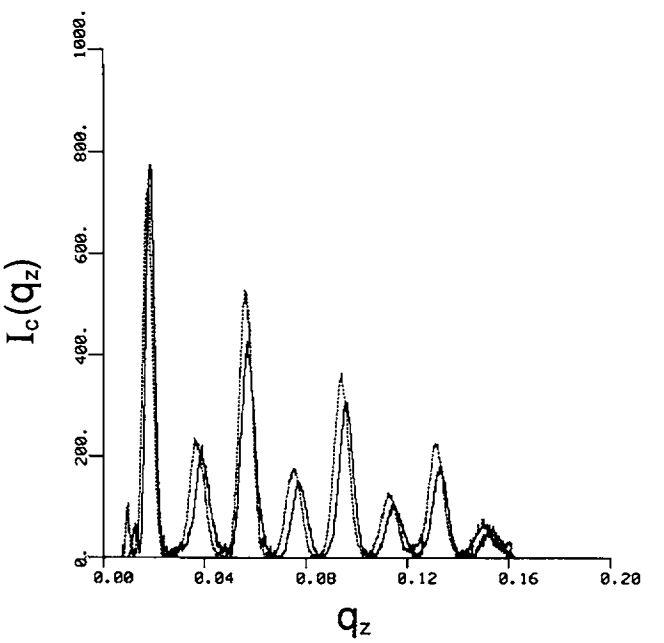

FIGURE 1 The corrected meridional intensity functions for ultrathin multilayer films consisting of four monolayers of arachidic acid and a monolayer of thioethyl stearate (TES), shown with a solid line, and four monolayers of arachidic acid, a monolayer of TES, and a covalently bound monolayer of yeast cytochrome *c*, shown with a dotted line.

having four monolayers of arachidic acid and a surface lipid monolayer of TES (AAAA/TES), and four monolayers of arachidic acid, a surface lipid monolayer of TES, plus a covalently bound layer of yeast cytochrome *c* (AAAA/TES/cyto). The corrected intensity functions of Fig. 1 are indicative of diffraction from asymmetric multilayers of finite extent, as discussed previously (5).

The one-dimensional Fourier transform of the corrected meridional intensity function yields the autocorrelation functions of the multilayer relative electron density profile, which requires no phase information. The autocorrelation functions for each set of intensity data were calculated; these autocorrelation functions are approximately pseudoperiodic in d_o, where d_o is the profile extent of one AA bilayer, and decay monotonically to zero with increasing $|z|$ for $|z| > D_n$, where D_n is the extent of the multilayer profile composed of n monolayers, so that $D_n \simeq nd_o/2$. Small amplitude, low spatial frequency oscillations centered about the zero baseline extend beyond $|z| = \pm D_n$, due to the truncation of the data for $q_z < q_{z[min]}$, and to errors in the corrected intensity function dominated by errors in background scattering correction at low q_z.

By comparing the autocorrelation functions calculated for the AAAA/TES multilayer (Fig. 2, *top*), and the AAAA/TES/cyto multilayer (Fig. 2, *bottom*), the effects of the bound yeast cytochrome *c* surface layer on the multilayer profile structure are indicated. The regions of the autocorrelation functions over the range of the horizontal arrows are most sensitive to the presence or absence of bound cytochrome *c*; they are dominated by the correlations of the relative electron density profile features of the multilayer's first monolayer (fatty-acid) on the alkylated glass substrate with the last surface monolayer (TES) ± cytochrome *c*. We note that significant features exist within this region of the autocorrelation function for the AAAA/TES cyto multilayer, which are absent in the comparable regions of the autocorrelation function for the AAAA/TES multilayer (Fig. 2).

The box refinement procedure, which utilizes the simple boundary condition that the multilayer relative electron density profile is zero outside of a box of length D_n, has been effectively applied to diffraction data from finite systems to produce correct multilayer profiles (5, 10). This technique is an iterative procedure which begins with the application of a phase for each point in q_z, derived from the Fourier transform of an arbitrary trial function, to the modulus of the experimental structure factor; a trial function such as a ramp function, or a phase-shifted sinusoidal function, will thus initiate the iteration with noncentrosymmetric phases. For the results presented here, it was found that a number of arbitrary trial functions produced multilayer relative electron density profiles generally containing the expected features of fatty acid bilayer/monolayer profiles (e.g., electron deficient terminal methyl group troughs and electron dense carboxyl group peaks separated by dimensionally appropriate intermediate density methylene chain groups); in addition, these profiles have the proper number of monolayers, as independently verified by the multilayer profile autocorrelation functions.

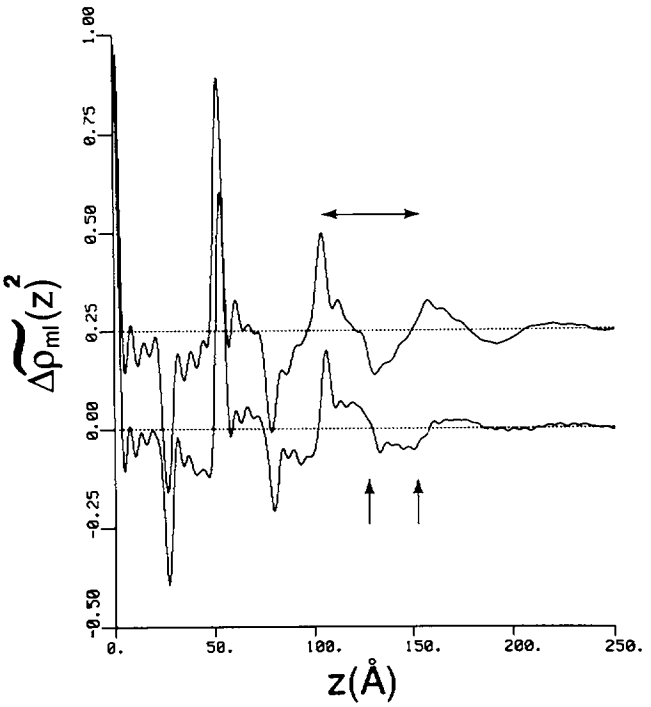

FIGURE 2 The multilayer profile autocorrelation (or generalized Patterson) functions calculated from the corrected intensity functions of Fig. 1, for ultrathin multilayer films consisting of four monolayers of arachidic acid and a monolayer of thioethyl stearate (TES) (*upper figure*) and four monolayers of arachidic acid, a monolayer of TES, and a covalently bound monolayer of yeast cytochrome *c* (*lower figure*). The region of the autocorrelation functions indicated by the horizontal arrow is most sensitive to the presence or absence of bound cytochrome *c*, as these regions contain only the correlations of the electron density profile features of the multilayer's first monolayer (fatty-acid on the alkylated glass substrate) with the last surface monolayer (TES) ± cytochrome *c*.

Figs. 3, *A* and *B* show the multilayer relative electron density profiles generated after 10 iterations of the box refinement utilizing the corrected intensity functions of Fig. 1, *A* and *B*, respectively. For these figures, a phase-shifted cosine trial function with a wavelength of $\sim 2D_n$ and the box constraint of $\sim D_n$ obtained from the multilayer profile autocorrelation functions, were applied. The relative electron density profiles for both the AAAA/TES multilayer and the AAAA/TES/cyto multilayer were thus calculated using the same trial function and boundary constraint (Fig. 3).

In a similar manner to the AAAA/TES and AAAA/

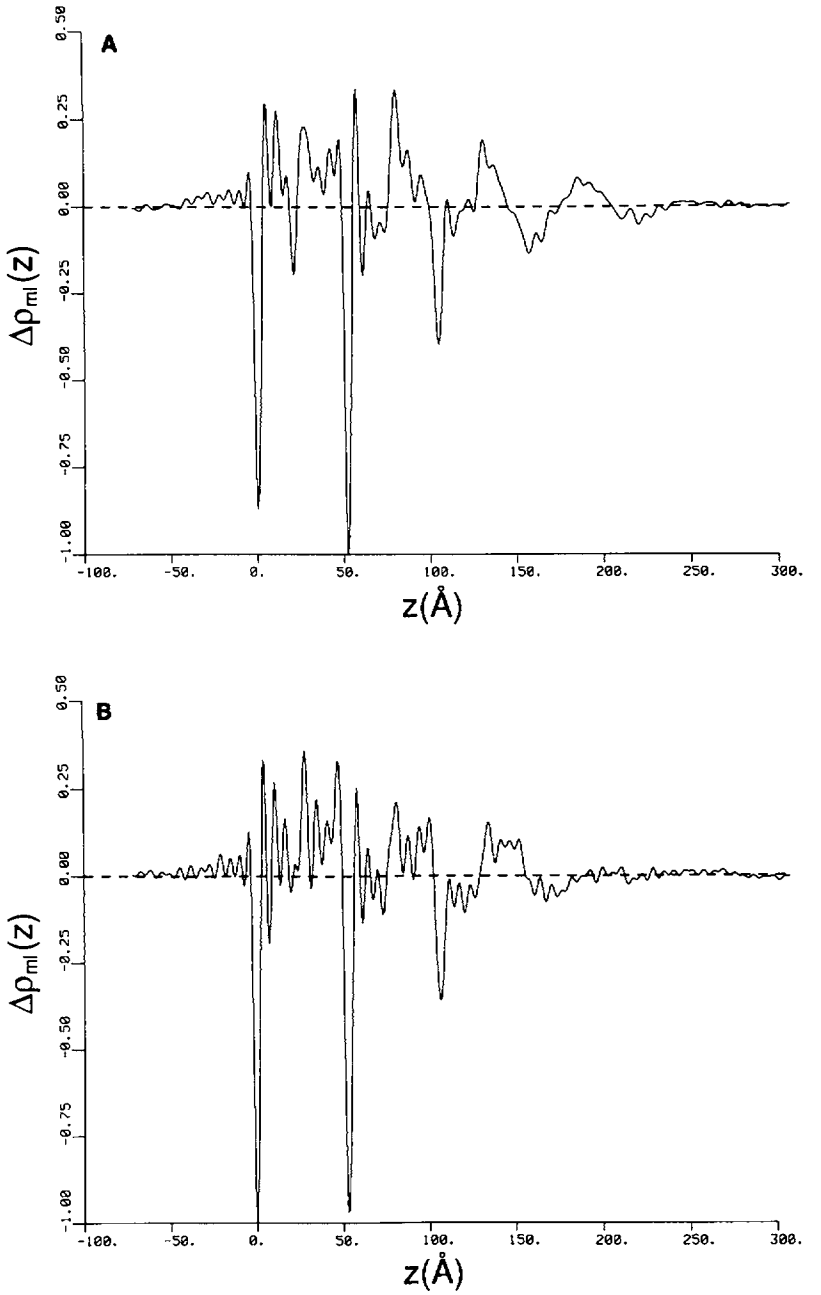

FIGURE 3 The multilayer relative electron density profiles $\Delta\rho_{ml}(z)$ for nonperiodic multilayer lattices as derived via the box-refinement phasing method, showing $\Delta\rho_{ml}(z)$ for an ultrathin film consisting of (*A*) four monolayers of arachidic acid and a monolayer of thioethyl stearate (TES); (*B*) four monolayers of arachidic acid, a monolayer of TES, and a covalently bound monolayer of yeast cytochrome *c*. The alkylated glass substrate would appear to the left of $z = 0$ *A*, while the TES polar headgroup in *A* and *B* occurs at $z = 104$ A.

TES/cyto multilayers, the relative electron density profiles of the following ultrathin multilayer films were calculated: AAAAA, AAAAA/cyto, AAAA/PS (where PS = dimyristoyl phosphatidylserine), and AAAA/PS/cyto. Upon inspection of these six electron profiles, it was found that the profile structure of the four underlying arachidic acid monolayers deposited onto the OTS substrate surface were nearly identical (not shown). The major features in common to all these profiles included well-defined terminal methyl group troughs at $z \cong 0, 55$, and 110 A and carboxyl group peaks at $z \cong 30$ and 85 A thereby corresponding to the expected profile extent of

the AA bilayer of $d_o \simeq 55$ A (for example, see Fig. 3). The surface lipid monolayers of either arachidic acid, phosphatidylserine, or TES exhibited distinctive features characteristic of monolayer profile structures, namely a terminal methyl trough at $z \simeq 110$ A, and a polar headgroup peak at $z \simeq 140$ A with an intervening chain methylene group region.

More importantly, there were significant structural changes which occurred both within and outside of the surface lipid monolayer and the next underlying lipid monolayer upon binding of yeast cytochrome *c* in all cases. To depict these differences, Figs. 4, *A–C*, show only these first two monolayers at the multilayer surface (respectively, two arachidic acid monolayers, arachidic acid/PS, and arachidic acid/TES) with and without cytochrome *c* bound to the surface lipid monolayer. The phosphatidylserine and the TES surface monolayer profiles (the top of Figures 4, *A* and *B*, respectively) both exhibit relatively sharp polar headgroup peaks at $z \simeq 135$ A, with the TES profile having an additional shoulder of electron density at the surface (probably due to the electron dense thiol moiety; see Discussion). The

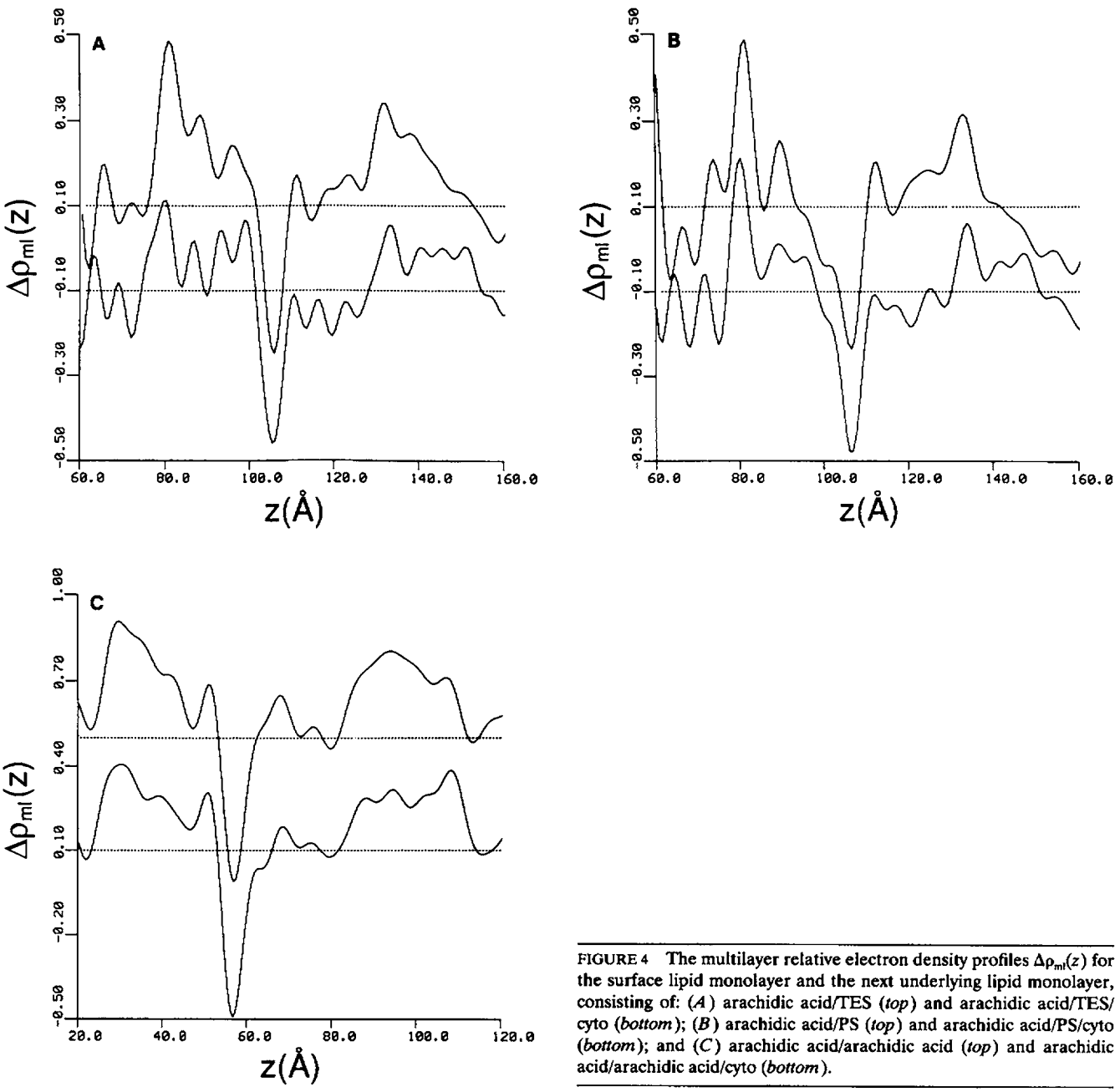

FIGURE 4 The multilayer relative electron density profiles $\Delta\rho_{ml}(z)$ for the surface lipid monolayer and the next underlying lipid monolayer, consisting of: (*A*) arachidic acid/TES (*top*) and arachidic acid/TES/cyto (*bottom*); (*B*) arachidic acid/PS (*top*) and arachidic acid/PS/cyto (*bottom*); and (*C*) arachidic acid/arachidic acid (*top*) and arachidic acid/arachidic acid/cyto (*bottom*).

profile structure of the arachidic acid surface (Fig. 4 *C*, *top profile*) exhibits a broad carboxyl group peak between 85 A $< z <$ 105 A. When a monolayer of yeast cytochrome *c* is bound to the surface lipid monolayer of each of the three multilayer samples, an additional broad electron density feature appears at the surface of each of the multilayer profile structures (bottom profiles of Figs. 4, *A–C*). It has been shown previously that this additional feature is due to the electron density of cytochrome *c* bound to the surface lipid monolayer (5, 6). In all cases, the electron density feature of the bound cytochrome *c* is nearly equal in amplitude to the electron density of the adjacent lipid polar headgroup peak; the full-width at half maximum for the cytochrome *c* electron density feature is 25–30 A.

It has also been observed that the average electron density of the hydrocarbon chain methylene group region of the surface lipid monolayer decreases upon binding of a monolayer of cytochrome *c*. This phenomena is especially evident when comparing the surface lipid monolayers of the top of Figs. 4, *A* and *B* to the bottom of Figs. 4, *A* and *B*, respectively. In addition, Fig. 3 *B* shows that the average electron density of the hydrocarbon chain methylene group region of the surface lipid monolayer with a bound monolayer of cytochrome *c* is significantly lower than the corresponding hydrocarbon chain methylene group regions of all four underlying lipid monolayers. Finally, Table 1 shows that an increase in the terminal methyl group trough to polar headgroup peak distance occurs within the surface lipid bilayer, and especially for the surface lipid monolayer, upon binding cytochrome *c* to the surface of the lipid multilayers.

DISCUSSION

It is well established that cytochrome *c* binding to lipid films is highly dependent on the lipid polar headgroup charge, as determined by the experiments varying ionic strength and pH (2). For example, our previous studies on cytochrome *c* binding to ultrathin lipid multilayers of arachidic acid showed that the interaction was primarily electrostatic. Although the binding of cytochrome *c* to simple fatty acids is primarily a nonspecific electrostatic interaction, we have demonstrated in related experiments that the lateral motion of cytochrome *c* is highly restricted in the plane of the multilayer surface (as indicated from the protein lateral diffusion constant derived from fluoresence recovery after photobleaching [FRAP] experiments [4]). In addition, linear dichroism studies have shown that a high degree of orientation (as indicated from the distribution of tilt angles about the mean for its heme plane with respect to the membrane plane) occurs not only for cytochrome *c* that is covalently bound to TES and phosphatidylserine lipid surfaces, but also for cytochrome *c* that is electrostatically bound to arachidic acid surfaces (4).

The x-ray diffraction data presented in this study confirms our previous results, demonstrating that meridional diffraction can be utilized to determine the profile structure of ultrathin lipid multilayers with a bound surface monolayer of protein. Significant changes occurred in the corrected intensity data for the ultrathin lipid films upon cytochrome *c* binding (Fig. 1); these changes are reflected in the multilayer profile autocorrelation functions of Fig. 2, and in the electron density profiles of Fig. 3, *A* and *B*. A comparison of the features that appear in the region of 120 A $< |z| <$ 150 A in the autocorrelation functions of Fig. 2 indicates that additional electron density appears on the surface of the thin films due to the addition of covalently bound cytochrome *c* (5). These autocorrelation functions are independent of phase information and can be thus used in support of the changes seen in the multilayer relative electron density profiles, which were calculated using intensity and phase information. In an analogous fashion, a comparison of the relative electron density profiles with and without covalently bound cytochrome *c* in Fig. 3, *A* and *B*, shows that additional positive relative electron density features appear at the surface of the multilayers having bound protein which have been previously identified as electron density due to a monolayer of cytochrome *c* (5).

In a previous investigation of the structure of ultrathin lipid films, it was found that the arachidic acid monolayer at the monolayer/air surface of the multilayer profile was disordered (11). Indeed, the surface monolayer of arachidic acid shown as the top profile structure of Fig. 4 *C* is indicative of the type of disorder described previously, namely that the surface carboxyl group electron density is distributed over a larger region of *z* than for the nonsurface arachidic acid monolayers; in addition, the average distance between the methyl group trough to the carboxyl group peak is greater for the surface vs. the nonsurface arachidic acid monolayers (Fig. 4 *C*). This does not seem to be the case when the surface monolayer consists of either phosphatidylserine (PS) or TES; the distance between the methyl group trough to the polar headgroup peak is nearly equal for the PS or TES surface monolayers versus the nonsurface arachidic acid monolayers (Table 1) and the top profiles of Figs. 4, *A* and *B*, also exhibit relatively little disorder in the outermost polar headgroup peak. Also note that there is an additional positive relative electron density feature at the surface of the TES monolayer outside of the major polar headgroup peak (top profile of Fig. 4 *B*); this would be an expected feature due to the sulfhydryl

TABLE 1 **Distance between methyl group trough to carboxyl group peak (in Angstroms)**

Sample	Monolayer	
	#1	#2
A. AAAA/PS	25.4	25.3
AAAA/PS/cyto	27.4	26.8
B. AAAA/TES	25.5	25.3
AAAA/TES/cyto	27.5	26.3

PS, Dimyristoyl phophatidylserine; TES, Thioethyl stearate; A, Arachidic acid. Monolayer 1: Surface lipid monolayer (PS or TES, respectively). Monolayer 2: Next underlying monolayer (A).

of the thioethyl moiety extended normal to the surface plane. The absence of such an additional feature at the surface of the PS monolayer profile indicates that the entire phosphatidyl serine moiety lies within the one polar headgroup peak (at this limited resolution).

Under conditions where cytochrome *c* would electrostatically bind to a charged lipid headgroup, other investigators have shown that cytochrome *c* induces significant surface pressure changes in lipid monolayer films (1); such surface pressure changes have been interpreted as resulting from penetration of hydrophobic residues of the protein among the lipid hydrocarbon chains (1, 3). Although x-ray diffraction studies of cytochrome *c*/lipid systems utilizing unoriented multilamellar lipid vesicles have suggested this same interpretation (13), our previous strcutural studies provided results definitively showing such interaction of cytochrome *c* with a surface lipid monolayer. Electron density profiles indicated that the cytochrome *c* monolayer penetrates the hydrophillic lipid polar headgroup surface to the level of the hydrocarbon chains. It is evident from the electron density profiles shown in this study, and Table 1, that deformation of the lipid bilayer also occurs upon covalent binding of yeast cytochrome *c*. It is possible, given the information of Table 1 and the changes in the relative electron density of the chain methylene group region, that the tilt of the lipid alkyl chains relative to the monolayer plane decreases thereby increasing the area/chain in the monolayer plane, and thereby allowing penetration of the protein. It should also be noted that some deformation of the tertiary structure of cytochrome *c* (12) may necessarily occur, allowing its penetration of the lipid monolayer surface.

Studies have begun in which integral membrane proteins have been bound to the cytochrome *c* covalently attached to the surface of an ultrathin lipid multilayer film or a self-assemble monolayer surface (14). It has been found that meridional x-ray diffraction can detect the presence of a photosynthetic reaction center monolayer (an integral membrane protein) electrostatically bound to the covalently attached cytochrome *c* monolayer (14); further studies are underway to determine the profile and in-plane structure of this integral membrane protein complex with the covalently attached cytochrome *c*, and to demonstrate the biochemical viability of the cytochrome *c*/reaction center complex.

REFERENCES

1. Quinn, P. J., and R. M. C. Dawson. 1969. Interactions of cytochrome *c* and C14-carboxymethylated cytochrome *c* with monolayers of phosphatidylcholine, phosphatidic acid, and cardiolipin. *Biochem. J.* 115:65–75.
2. Nicholls, P. 1974. Cytochrome *c* binding to enzymes and membranes. *Biochim. Biophys. Acta.* 346:261–310.
3. Steinemann, A., and P. Lauger. 1971. Interaction of cytochrome *c* with phospholipid monolayers and bilayer membranes. *J. Membr. Biol.* 4:74–86.
4. Pachence, J. M., S. Amador, G. Maniara, J. Vanderkoii, P. L. Dutton, and J. K. Blasie. 1990. The orientation and lateral mobility of cytochrome *c* on the surface of ultrathin lipid multilayer flims. *Biophys. J.* 58:379–389.
5. Pachence, J. M., and J. K. Blasie. 1987. The location of cytochrome *c* on the surface of ultrathin lipid multilayer films using x-ray diffraction. *Biophys. J.* 52:735–747.
6. Pachence, J. M., R. Fischetti, and J. K. Blasie. 1989. Location of heme-Fe atoms within the profile structure of a monolayer of cytochrome *c* bound to the surface of an ultrathin lipid multilayer film. *Biophys. J.* 56:327–337.
7. Louie, G. V., W. L. B. Hutcheon, and G. D. Brajer. 1988. Yeast Iso-1-cytochrome *c*: A 2.8 A Resolution three-dimensional structure determination. *J. Mol. Biol.* 199:295–314.
8. Sagiv, J. 1980. Organized monolayers by adsorption. I. Formation and structure of oleophobic mixed monolayers of solid surfaces. *J. Am. Chem. Soc.* 102:92–98.
9. Ganog, B. R., and R. M. Bell. 1984. Transmembrane movement of phosphatidyl- glycerol and diacylglycerol sulfhydryl analogues. *Biochemistry.* 23:4977–4983.
10. Skita, V., M. Filipkowski, A. F. Garito, and J. K. Blasie. 1986. Profile structures of very thin multilayers by x-ray diffraction using direct and refinement methods of analysis. *Phys. Rev. B.* 34:5826–5837.
11. Skita, V., W. Richardson, M. Filipkowski, A. Garito, and J. K. Blasie. 1986. Overlayer-induced ordering of the disordered surface monolayer in Langmuir-Blodgett multilayer thin films. *J. Physique.* 47:1849–1855.
12. Dickerson, R. E., and R. Timkovich. 1975. Cytochromes *c*. *In* The Enzymes P. D. Boyer, editor. 3rd ed. Academic Press, NY. 11:395–544.
13. Shipley, G. G., R. B. Leslie, and D. Chapman. 1969. X-ray diffraction study of the interaction of phospholipids with cytochrome *c* in the aqueous phase. *Nature (Lond.).* 222:561–562.
14. Amador, S.M., J. M. Pachence, J. P. McCauley, Jr., A. B. Smith, III, P. H. Dutton, and J. K. Blasie. 1990. X-Ray diffraction studies of protein monolayers bound to self-assembled monolayers. *Mat. Res. Soc. Symp. Proc.* 177:393–398.